Heliyon 7 (2021) e06352

Contents lists available at ScienceDirect

Heliyon

journal homepage: www.cell.com/heliyon

Research article

# Nutrient starvation induces apoptosis and autophagy in C6 glioma stem-like cells

Wanna Sa-nongdej [a], Sukumal Chongthammakun [b,c], Chanchai Songthaveesin [c,*]

[a] Ramathibodi School of Nursing, Faculty of Medicine Ramathibodi Hospital, Mahidol University, Bangkok, 10400, Thailand
[b] Department of Anatomy, Faculty of Science, Mahidol University, Bangkok, 10400, Thailand
[c] Center for Neuroscience, Faculty of Science, Mahidol University, Bangkok, 10400, Thailand

ARTICLE INFO

*Keywords:*
C6 glioma stem cells
Nutrient starvation
Apoptosis
Autophagy

ABSTRACT

Glioblastoma is a severe cancer with extremely poor survival. Its treatment typically involves a combination of surgery, chemotherapy, and radiation therapy. However, glioma stem-like cells (GSCs)-a subpopulation of tumor-propagating glioblastoma cells—cause post-treatment recurrence and are a major factor in the poor prognosis of the disease. GSCs have higher proliferation than non-GSCs and are more resistant to invasive chemotherapy and radiotherapy. In this study, we subjected GSCs to nutrient starvation (deprived of glucose, glutamine, and calcium) to determine whether cell death can be triggered as a potential strategy to improve treatment outcomes. Flow cytometry revealed that 35.1%, 96.1%, and 99.9% of starved GSCs underwent apoptosis on days 1, 3, and 5, respectively, along with nearly 100% autophagy on all three days. Western blots detected cleaved caspase-3 (an apoptosis marker) and phospho-beclin 1, LC 3B-I, LC 3B-II (autophagy markers) in C6 GSCs after nutrient starvation for 1, 3, 4, and 5 days. Transmission electron microscopic observation of GSC ultrastructure after starvation treatment revealed that compared with control GSCs, starved cells had more pyknotic nuclei, membrane bleb, swollen endoplasmic reticulum, degenerative mitochondria, lipid droplets, and microvilli loss. Thus, nutrient starvation stresses cells by increasing free radicals. Cell stress opens more channels between mitochondria and endoplasmic reticulum. This study demonstrated that nutrient starvation decreases proliferation by approximately 81%, while increasing apoptosis (99.9%) and autophagy (94.6%) in C6 GSCs by the fifth day. Nutrient starvation of GSCs may, therefore, be an effective therapeutic strategy that can trigger apoptotic and autophagic metabolic reprogramming in cancer cells.

## 1. Introduction

Glioblastoma is a type of cancer originating from glial-type cells (e.g., astrocytes, oligodendrocyte progenitor cells, and glioblastoma stem-like cells), found in about 15% of brain tumors. Overall incidence rate of all brain tumors is 10.82 (95% CI: 8.63–13.56) per 100,000 person-years [1]. Glioblastoma is a severe disease, with 97% of patients surviving for only approximately 12–15 months after diagnosis [2].

Glioblastoma treatment typically involves surgery after chemotherapy and radiation therapy. However, chemoresistant glioma stem-like cells (GSCs), a subpopulation of tumor-propagating glioblastoma, frequently cause post-treatment tumor recurrence [3, 4]. These cells have the potential for unlimited growth, self-renewal, and multilineage differentiation to neurons, astrocytes, and oligodendrocytes [3, 4].

Radio-chemotherapy inhibits cell division and DNA replication. However, while this treatment does decrease GSC division and the cells do enter senescence, these cells possess the ability for subsequent restoration of viability, making them resistant to treatment. Stress may decrease GSCs and limit cancer stem cell renewal [3, 4]. For example, glucose deprivation for over 48 h activated autophagy in human transformed fibroblasts, but other starvation conditions did not induce the same effect [5]. Cancer cells convert glucose into lactate mostly through glycolysis [6], while glutamine is an essential source of anaplerotic intermediates for the tricarboxylic acid cycle. Therefore, cancer cells still use ATP production. In particular, GSCs proliferate more than non-GSCs and thus have relatively higher glucose metabolic rates, suggesting that they use different mitochondrial biosynthesis and metabolic pathways from those of non-GSCs or differentiated glioma cells. Cancer cells require 100 times more glutamine than they do other amino acids [7]. A

* Corresponding author.
*E-mail address:* chanchai.son@mahidol.ac.th (C. Songthaveesin).

https://doi.org/10.1016/j.heliyon.2021.e06352
Received 1 August 2020; Received in revised form 24 September 2020; Accepted 19 February 2021

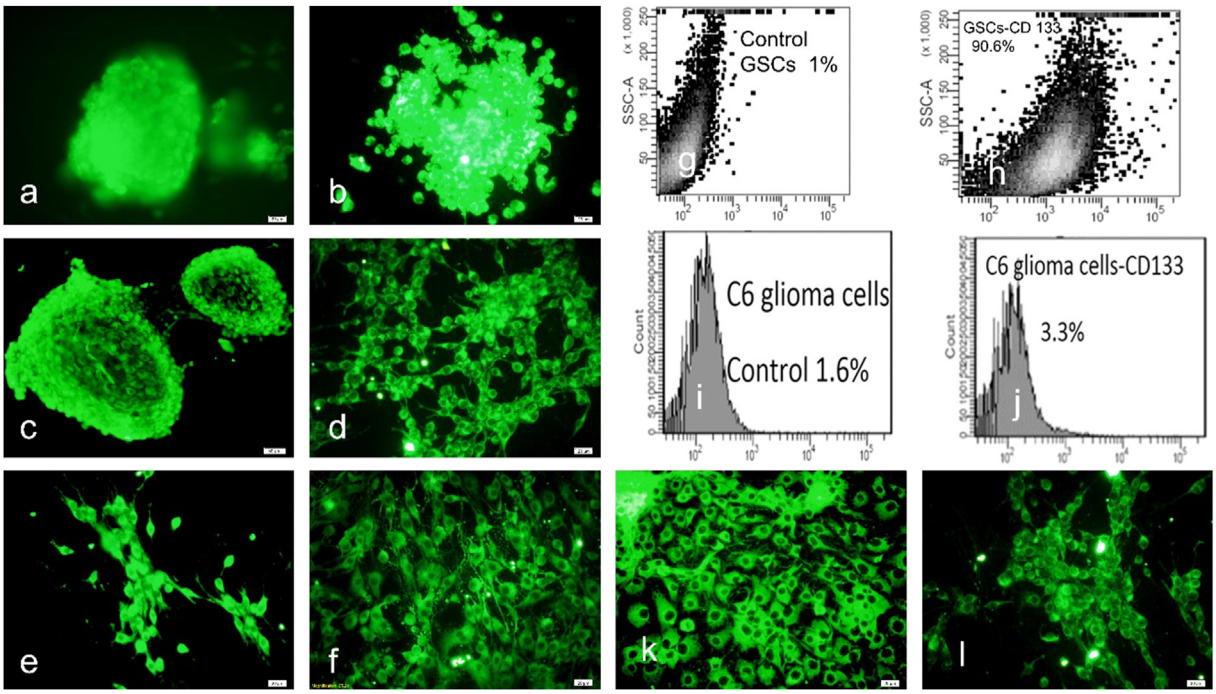


**Figure 1.** C6 gliospheres were induced using 20 ng/mL EGF, 20 ng/mL bFGF, and B27. Cells were confirmed as glioma stem-like cells (GSCs) using (a) CD 133 (green), (b) CD 44 (green), and (c) nestin (green). C6 GSCs can differentiate into (d) astrocytes (GFAP, green), (e) oligodendrocytes (MOG, green), and (f) neurons (synaptophysin, green). Flow cytometry of CD 133 staining showed that 90.6% of gliospheres in C6 GSCs were CD 133-positive (h and g as a control), while 3.3% C6 (non-GSC) glioma cells were CD 133-positive (j and i as a control). GFAP (green) in C6 rat glioma cells (non-GSCs) (k) compared with differentiated C6 rat GSCs under the serum-medium condition (l) on day 7. a-b, d-f, k-l scale bar = 20 μm and c, scale bar = 50 μm.

lack of cellular calcium has been implicated in the induction of apoptosis and autophagy [8, 9].

Programmed cell death (apoptosis, necrosis, and autophagy) involves the expression and regulation of multiple genes [10]. Apoptosis is characterized by changes in the morphological and biochemical hallmarks of GSCs, such as cell shrinkage, pyknotic nuclei, nuclear fragmentation, and membrane blebbing [11]. During apoptosis, caspases cleave cells and pack the remnants into apoptotic bodies as a mechanism to avoid immune stimulation. The mechanism underlying the radioresistance of GSCs is likely the upregulation of anti-apoptotic proteins and DNA repair enzymes. Successful necrotic activation may have major biological consequences in GSCs and could limit their tumorigenic potential, including the induction of an inflammatory response [12, 13, 14].

Autophagy is an adaptation to nutrient starvation, wherein cells self-digest. Autophagy is induced by the activity of PI3K phosphatidylinositol 3-kinase/AMPK (adenosine monophosphate-activated protein kinase) and other nutrient-sensing pathways [15, 16].

In this study, we subjected GSCs to nutrient (glucose, glutamine, calcium) starvation, with the aim of characterizing their cell-death-related response. We examined flow cytometry indicators of apoptosis and autophagy. We also detected various marker proteins for the two processes, specifically, cleaved caspase-3 (apoptosis) and phospho-beclin 1, LC 3B-I, and LC 3B-II (autophagy). Finally, we examined the morphology of starved GSCs during apoptosis and autophagy.

These findings will improve our understanding of GCSs and their response to clinical treatments, benefiting the development of therapies

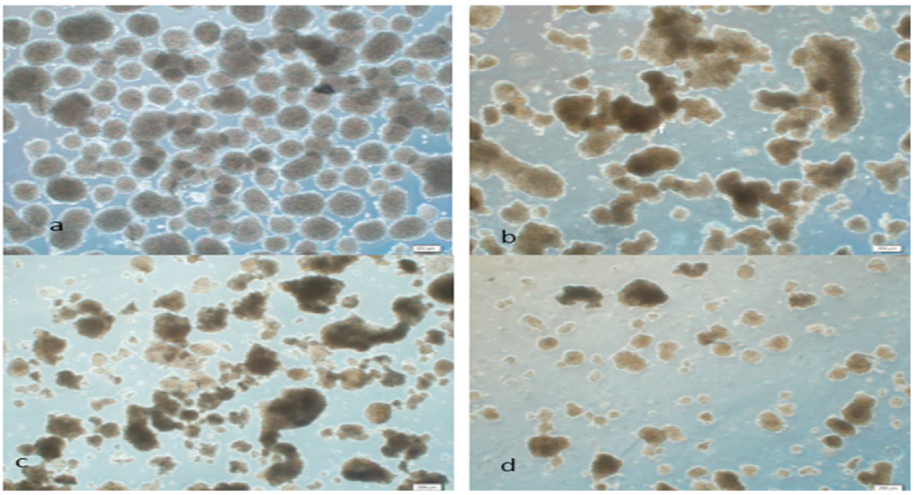


**Figure 2.** Representative micrographs (a–d) of C6 glioma stem-like cells (GSCs) after 1 (b), 3 (c), and 5 (d) d of nutrient starvation (no glucose, glutamine, or calcium) compared with control GSCs cultured in nutrient-rich medium (a). scale bar = 200 μm.

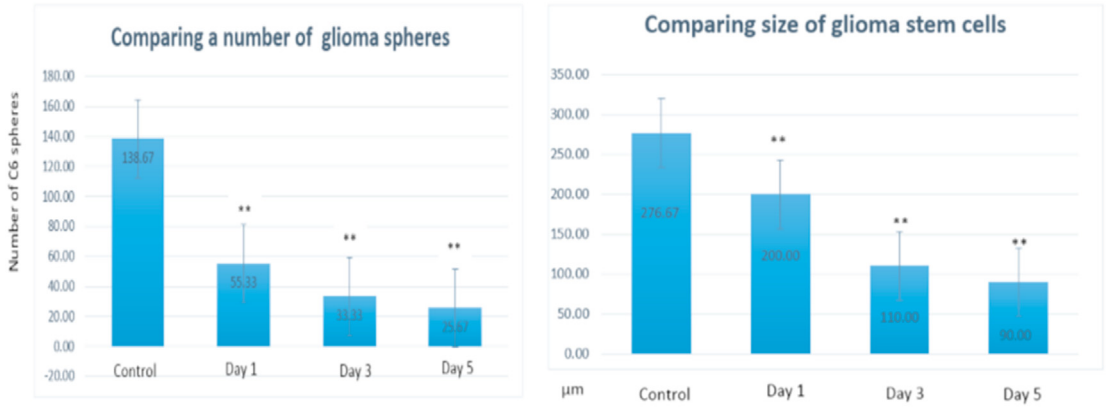


**Figure 3.** Number and size of C6 glioma stem cells after nutrient starvation on days 1, 3, and 5 compared with control gliospheres cultured in glioma stem cell medium.

that are more specific and effective. By employing the mechanisms of nutrient starvation, we may see dramatic enhancements in treatment outcomes for glioblastomas.

## 2. Materials and methods

C6 gliospheres were induced to generate GSCs. Briefly, C6 glioma cells (Cell Lines Service, Denmark) were plated onto coverslips in a six-well plate containing Dulbecco's Modified EagleMedium(DMEM):Nutrient Mixture F-12 (1:1; Gibco, USA) supplemented with 10% fetal bovine serum (FBS, United Kingdom). Cells were placed in a humidified atmosphere of 5% $CO_2$ at 37 °C until confluent. Confluent cells were dissociated using 0.25% trypsin-EDTA (Gibco) solution and cultured in glioma stem cell medium, comprising neurobasal medium (NBM) supplemented with B27 (1X; Gibco), heparin (2 µg/mL), 20 ng/mL recombinant human basic fibroblast growth factor (bFGF, Sigma, USA), and 20 ng/mL recombinant human epidermal growth factor (hEGF, Sigma). Gliospheres were plated in a six-well plate, then stored in a 5% $CO_2$ incubator at 37 °C, with the medium changed every 3 d. Upon reaching >100 µm in diameter, C6 gliospheres were subjected to nutrient starvation using a non-glucose, non-glutamine, non-calcium medium (SILAC [stable isotope labeling with amino acids in cell culture] Advanced DMEM/F-12 Flex Media, Gibco) in a six-well plate and incubated (5% $CO_2$, 37 °C) for 0, 1, 3, and 5 d. Gliospheres were collected for subsequent analyses.

### 2.1. Flow cytometry

Flow cytometry assessed immunoreactivity of GSCs and C6 glioma cells to GSC marker CD 133. Untreated GSCs ($1 \times 10^6$ cells) and semi-confluent C6 glioma cells were washed with 500 µL (0.01 M) of phosphate-buffered saline (PBS), fixed in -20 °C absolute alcohol for 20 min, and treated with 5% bovine serum albumin for 20 min. Cells were then treated with 8 µL of CD 133-FITC antibody (E-bioscience, United Kingdom) and incubated in darkness for 1 h at room temperature. Secondary antibody Alexa Fluor®-488 was used as a control. The reaction was terminated with PBS. At least 10,000 cells were assessed on a FACScalibur flow cytometer (Becton Dickinson).

To detect early and late apoptosis, nutrient-starved C6 GSCs were stained with FITC-conjugated Annexin V and propidium iodide (PI) from Sigma. They were then subjected to the same flow cytometry procedures as described in the previous paragraph, except that 7 mL PI were added along with 8 µL of Annexin V-FITC for 1 h incubation in darkness at room temperature. The percentage of intact (Annexin V-/PI-), early apoptotic (Annexin V+/PI-), late apoptotic (Annexin V+/PI+), and necrotic

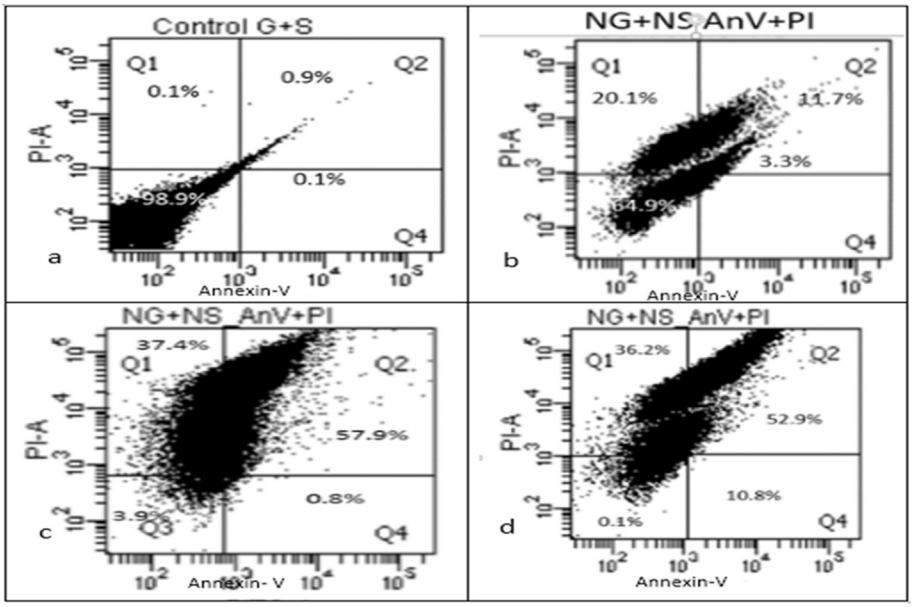


**Figure 4.** Flow cytometry of nutrient-starved glioma stem-like cells (GSCs) stained with Annexin V plus propidium iodide on days 1 (b), 3 (c), 5 (d), and control GSC medium (a). (b) Percentage of apoptotic cells after 1 day of nutrient starvation: Q1 (necrosis 20.1%), Q2 (late apoptosis 11.7%), Q3 (viable cells 64.9%), Q4 (early apoptosis 3.3%). (c) Percentage of apoptotic cells after 3 days of nutrient starvation: Q1 (necrosis 37.4%), Q2 (late apoptosis 57.9%), Q3 (viable cells 3.9%), Q4 (early apoptosis 0.8%). (d) Percentage of apoptotic cells after 5 days of nutrient starvation: Q1 (necrosis 36.2%), Q2 (late apoptosis 52.9%), Q3 (viable cells 0.1%), Q4 (early apoptosis 10.8%). (a) Percentage of apoptotic cells in control stem cell medium: Q1 + Q2 + Q4 (0.1% + 0.9% + 0.1% = 1.1% dead cells) and Q3 (viable cells 98.9%).

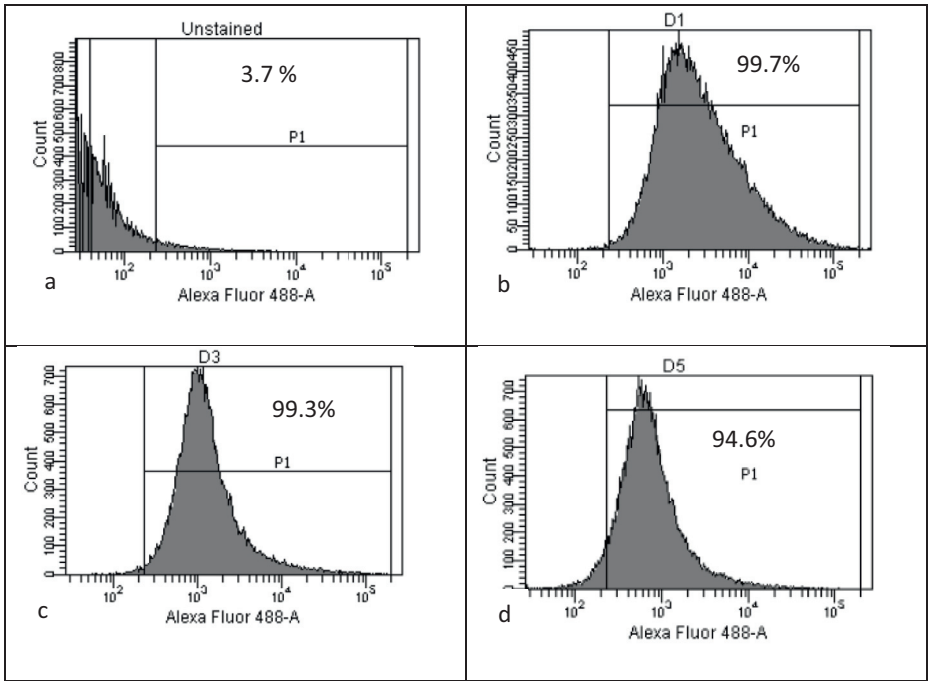


**Figure 5.** Flow cytometry to detect autophagy in GSCs treated with FITC-conjugated LC3B to induce nutrient starvation. (b) Day 1: 99.7%. (c) Day 3: 99.3%. (d) Day 5: 94.6%. (a) Control medium: 3.7%.

(Annexin V-/PI+) cells was calculated in FACSDiva version 6.1.1 (BD Biosciences).

For detecting autophagy, nutrient-starved cells were stained with FITC-conjugated LC3B (Sigma). Flow cytometry procedures remained the same as described in the first paragraph. Cells were then analyzed in FACSDiva.

### 2.2. Immunofluorescence staining

To detect proliferation, untreated GSCs were plated onto poly-L lysine (Sigma-Aldrich)-coated glass coverslips and incubated in DMEM/F12 with 10% FBS for 12 h. Gliospheres were washed three times with PBS, fixed in -20 °C absolute alcohol for 20 min, washed three times with PBS, and blocked with 5% bovine serum albumin (Sigma-Aldrich) for 20 min at room temperature. They were then immunostained with FITC-conjugated CD 133, CD 44, and nestin antibodies (E-bioscience) for 1 h in the dark. After washing with PBS, cells were incubated at 37 °C for 1 h with Alexa Fluor®-488 anti-mouse IgG antibody (1:100, Sigma) in darkness, washed three times with PBS, and mounted on microscope slides using glycerol mounting medium.

To detect differentiation, C6 GSCs were plated onto poly-L lysine (Sigma-Aldrich)-coated glass coverslips and incubated for 8 h in DMEM/

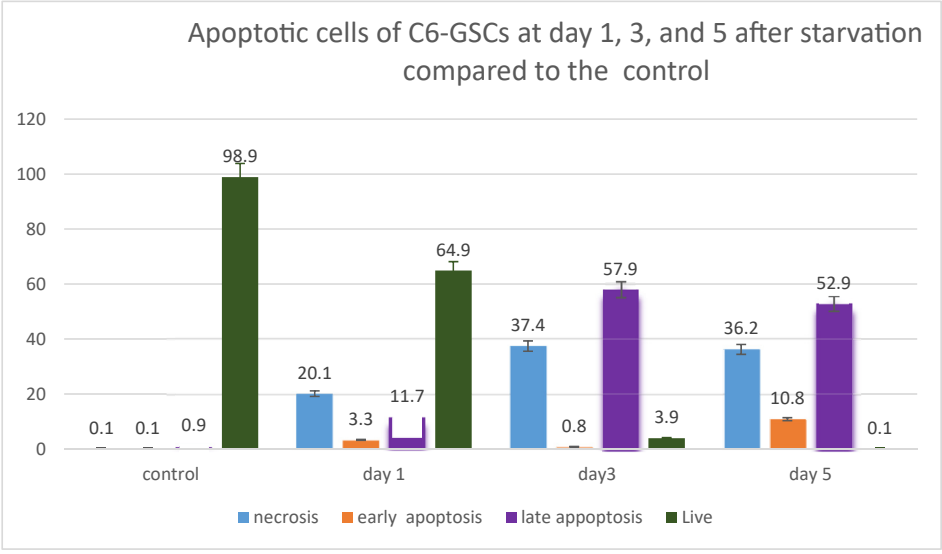


**Figure 6.** Flow cytometry of nutrient-starved C6 gliospheres on day 3 revealing 57.9% of cells in early apoptosis and 37.4% undergoing necrosis. Nutrient starvation significantly increased cell death rate compared with that in control conditions.

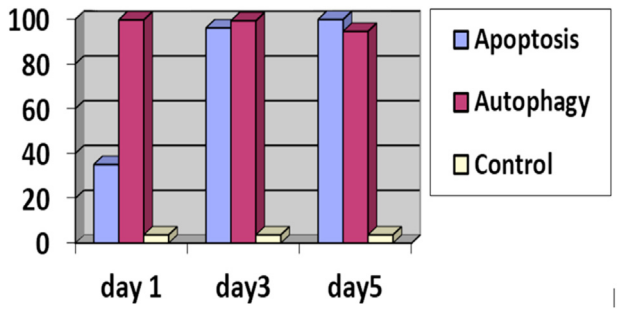


**Figure 7.** Comparison of control, apoptosis and autophagy on days 1, 3 and 5 after nutrient starvation by flow cytometry.

room temperature for 1 h with Alexa Fluor488 anti-mouse IgG antibody (1:100, Sigma), washed three times with PBS, mounted on microscope slides using glycerol mounting media, and examined under a fluorescence microscope (Olympus, IX71/IX51, Japan).

Next, the semiconfluent coverslip-cultured C6 cells were washed three times with PBS, fixed with -20 °C absolute alcohol for 20 min, and blocked using 5% bovine serum albumin for 20 min at room temperature. After washing again with PBS, they were stained for GFAP (1:100, mouse monoclonal IgG1; Santa Cruz, USA) for 1 h in the dark, before being washed with PBS. Next, cells were incubated at room temperature in the dark for 1 h with Alexa Fluor488 anti-mouse IgG antibody (1:100, Sigma). Finally, the cells were washed three times with PBS, mounted on microscope slides using glycerol mounting media, and examined under a

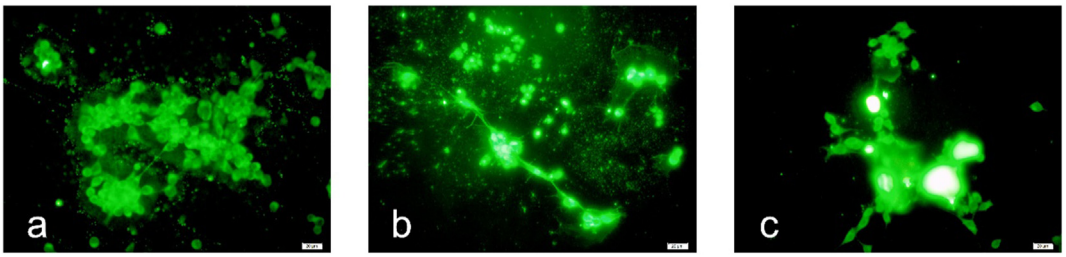


**Figure 8.** Autophagy detection in nutrient-starved gliospheres using anti-LC3B immunofluorescence. (a) Day 1. (b) Day 3. (c) Day 5. scale bar = 20 μm.

F-12 with 10% FBS. Differentiated C6 GSCs were washed three times in 500 μL of PBS (0.01 M). They were then fixed with -20 °C absolute alcohol for 20 min, washed three times in 500 μL of PBS (0.01 M), and blocked using 5% bovine serum albumin for 20 min at room temperature. For 1 h in darkness, cells were stained for glial fibrillary acidic protein (GFAP, 1:100 mouse monoclonal IgG1; Santa Cruz, USA), myelin oligodendrocyte protein (MOG 1:100, mouse monoclonal IgG1; Santa Cruz), and neurons (synaptophysin 1:100, mouse monoclonal IgG1; Dako, USA), then washed with PBS. Next, cells were incubated in darkness at

fluorescence microscope (Olympus, IX71/IX51).

For detecting autophagy, C6 GSCs were nutrient-starved for 0, 1, 3, and 5 days, washed three times with PBS, fixed with -20 °C absolute alcohol for 20 min, washed three times again with PBS, and blocked using 5% bovine serum albumin for 20 min at room temperature. After washing another three times with PBS, cells were incubated with rabbit anti-mouse LC3B (1:100 Sigma, primary antibody: autophagy) for 1 h in the dark. They were then rinsed with PBS to remove the antibody and then incubated again (1 h darkness at room temperature) with Alexa

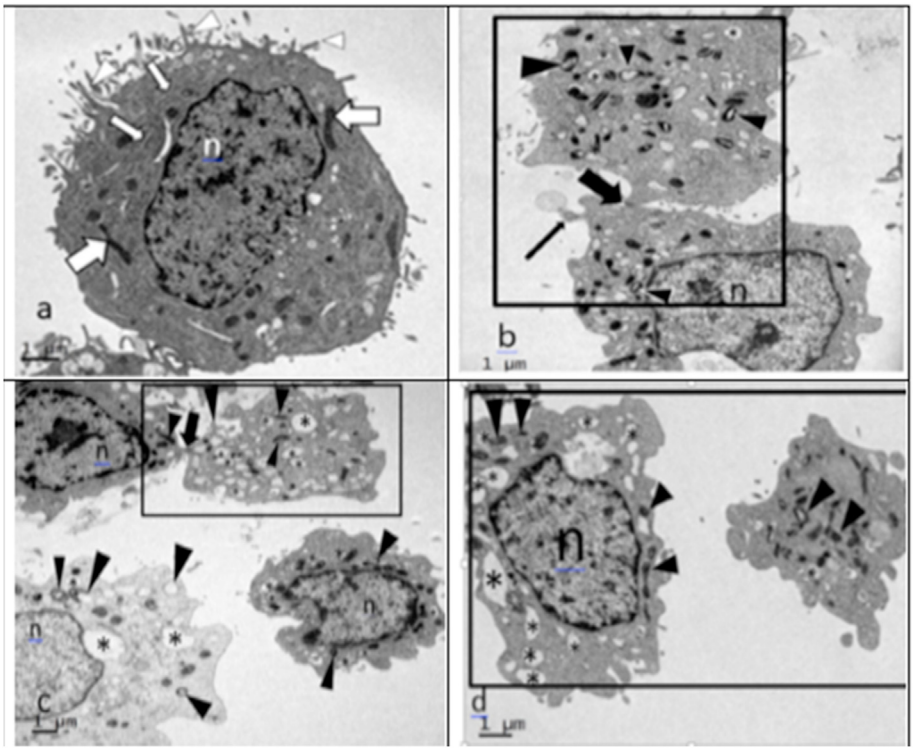


**Figure 9.** C6 glioma stem-like cell (GSC) morphology under the transmission electron microscope (TEM). (a) Control cell showing typical chromatin pattern in the nucleus (n), mitochondria (thick white arrow), endoplasmic reticulum (thin white arrow), and microvilli (white arrowheads). (b) Day 1 of nutrient starvation: damaged mitochondria (black arrowheads), membrane bleb (thin black arrow), intermediate junction or desmosome (thick black arrow), swollen endoplasmic reticulum (ER) profile (asterisks), and mitochondria-associated membrane (MAM, rectangle). (c) Day 3 of nutrient starvation: damaged mitochondria (black arrowheads), intermediate junction or desmosome (thick black arrow), swollen ER profile (asterisks), and MAM (rectangle). (d) Day 5 of nutrient starvation: damaged mitochondria (black arrowheads), swollen ER profile (asterisks), and MAM (rectangle). Right side, cellular process in GSC compared with control (a).

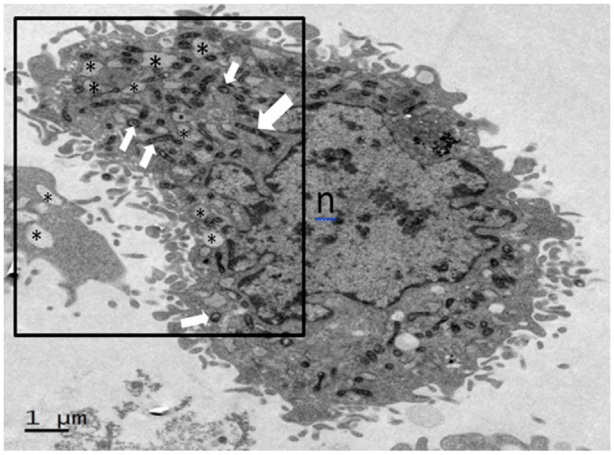


**Figure 10.** Glioma stem-like cells exhibiting multiple mitochondria-associated membranes (MAMs, rectangle). Several close associations between two or three swollen, rugous endoplasmic reticulum profiles (asterisks) with a damaged mitochondrion (arrow) can been seen at day 3 of nutrient starvation.

Fluor488 anti-mouse IgG antibody (1:100, Sigma). Subsequent to three more washes with PBS, cells were mounted on microscope slides using glycerol mounting medium and examined under a fluorescence microscope (Olympus, IX71/IX5).

### 2.3. Transmission electron microscopy (TEM)

Cells were fixed in 2.5% glutaraldehyde at pH 7.2 (at room temperature) for 24 h, postfixed using in a 0.1 M cacodylate buffer with 1% $OsO_4$ for 1 h, and stained with 0.2% uranyl acetate for 30 min. Cells were then dehydrated in a series of graded ethanol steps and finally embedded in Araldite. Ultrathin sections were double-stained with lead citrate and uranyl acetate, then viewed under a JEOL 1200 EX electron microscope.

### 2.4. Western blot

Cleaved caspase-3 and phospho-beclin 1, LC 3B-I, LC 3B-II proteins was analyzed. First, GSCs were plated into six-well plates. After nutrient starvation for 0, 1, 3, 4, and 5 days, cells were washed three times with PBS and collected via adding RIPA lysis buffer containing a protease inhibitor cocktail, then scraped off the wells. Lysates were centrifuged at 14,000 rpm at 4 °C for 15 min. The supernatant was collected, and protein concentration was measured using Bradford reagent at 595 nm. An equal amount of protein per sample was separated with 12% SDS-PAGE and transferred onto a nitrocellulose membrane (Bio-Rad Laboratories, CA, USA). Non-specific binding was blocked using 5% bovine serum albumin in TBS-T for 1 h at room temperature. Membranes were then incubated in 1:1000 dilutions at 4 °C overnight for mouse monoclonal primary antibody against cleaved caspase-3, phospho-beclin 1, LC 3B-I, and LC 3B-II (Santa Cruz Biotechnology). Another incubation followed with anti-mouse IgG secondary antibody (Zymed Laboratories, CA, USA). Membranes were developed using an ECL kit (Pierce Biotechnology).

### 2.5. Statistical analysis

Data were expressed as means ± standard deviations (SD), calculated from three independent replications. Differences between treated cells and controls were determined using the independent t-test. Significance was set at $p < 0.05$.

## 3. Results

### 3.1. Characteristics of C6 GSCs in gliospheres

Most C6 GSCs exhibited high CD 133 expression. The whole gliosphere was stained for CD 133, CD 44, and nestin (Figure 1a-c). Immunofluorescence staining revealed differentiated C6 GSCs, including astrocytes (Figure 1d), oligodendrocytes (Figure 1e), and neurons (Figure 1f). Flow cytometry showed that a CD 133-positive population was detected in 90.6% of C6 GSC gliospheres (Figure 1h and 1g [control]) and 3.3% C6 glioma cells (non-GSCs, Figures 1j and 1i [control]). We also compared GFAP in C6 glioma cells (Figure 1k) and differentiated rat C6 GSCs (Figure 1l) after 7 d of incubation in serum-containing medium. Nutrient starvation for 1, 3, and 5 d decreased gliosphere size and number compared with control. Treatment with nutrient starvation decreased proliferation in the surviving fraction of C6 GSCs, by 60.1% on day 1, 76% on day 3, and 81.5% on day 5 (Figures 2 and 3).

### 3.2. Effects of nutrient starvation on apoptotic cell death and autophagy in C6 GSCs

Flow cytometry revealed that after 1 d of nutrient starvation, 20.1% of cells underwent necrosis, 11.7% were in late apoptosis, 3.3% were in early apoptosis, and 64.9% remained viable (Figure 4). After 3 d, 37.4% underwent necrosis, 57.9% were in late apoptosis, 0.8% were in early

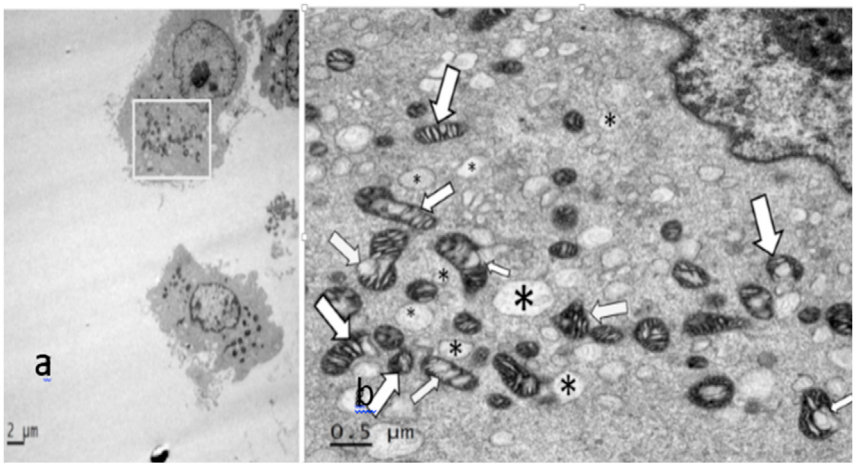


**Figure 11.** Glioma stem-like cells with a "mitochondria-associated membrane (MAM) network" of 15 direct inter-organellar close associations in mitochondria with swollen endoplasmic reticulum (ER; white rectangle) (a). (b) Enlargement of white rectangle in (a) showing a glioma stem-like cell with adjacent nuclei, swollen ER profiles (asterisk), and electron-dense vacuoles, damaged mitochondria, or mitophagy (arrow).

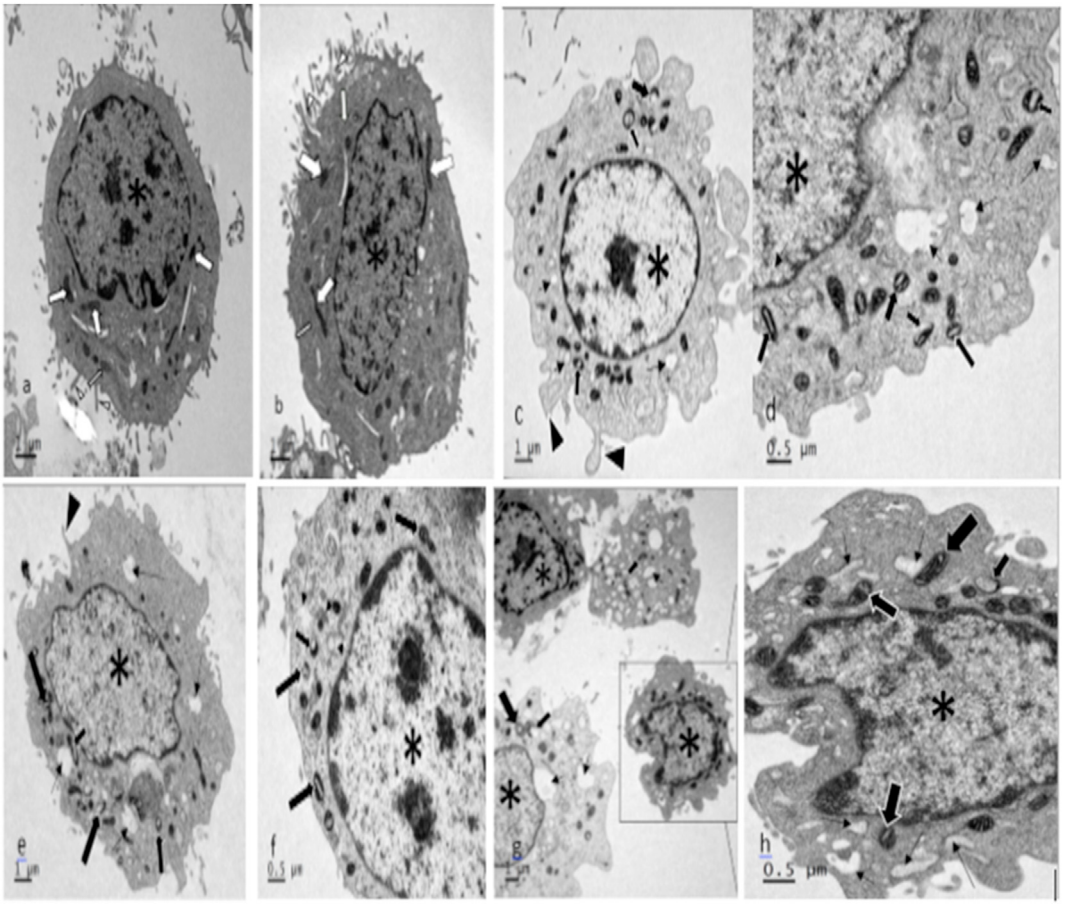


**Figure 12.** Ultrastructural morphology of glioma stem-like cells (GSCs). (a, b) Control gliospheres: nucleus (asterisks), mitochondria (white thick arrows), normal endoplasmic reticulum (ER; white thin arrows), and microvilli (white arrowheads). (c, d) C6 gliospheres on day 1 of nutrient starvation. (e, f) GSCs on day 3 of nutrient starvation. (g) GSCs on day 5 of nutrient starvation. (h) Enlargement of the rectangle in (g). Nucleus (asterisks), degenerated or damaged mitochondria or mitophagy (thick arrows), swollen and fused ER (thin arrows), and blebbing of apoptotic bodies (black arrowheads).

apoptosis, and 3.9% were viable (Figure 4). After 5 d, 36.2% underwent necrosis, 52.9% were in late apoptosis, 10.8% were in early apoptosis, and 0.1% were viable. In contrast, 1.1% control cells died and the remaining 98.9% were viable (Figure 4). Flow cytometry detected autophagy in 99.7% of nutrient-starved GSCs on day 1, 99.3% on day 3, 94.6% on day 5; only 3.7% of control GSCs underwent autophagy (Figures 5 and 6). We also performed another comparison of apoptosis and autophagy in control and nutrient-starved cells on days 1, 3, and 5 (Figures 7 and 8).

### 3.3. Effects of nutrient starvation on C6 GSC morphology

Nutrient-starved cells were smaller than control cells under TEM (Figure 9). Control GSCs had typical chromatin patterns, mitochondria, endoplasmic reticulum (ER), and microvilli. In contrast, after 1 d of nutrient starvation, we observed damaged mitochondria, membrane bleb, intermediate junction or desmosome, swollen ER profile, and mitochondria-associated membrane (MAM). After 3 days, we no longer observed membrane bleb, but all other characteristics remained. Intermediate junctions/desmosomes disappeared on day 5. Thus, GSCs had different cellular processes from those of control (Figure 9d). GSCs

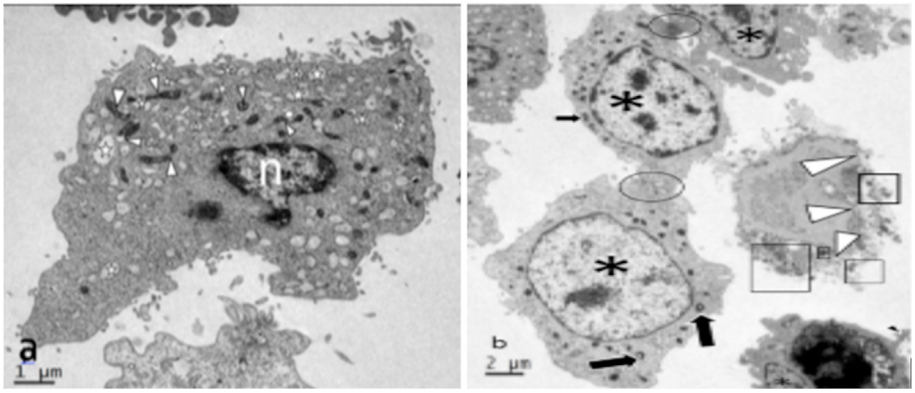


**Figure 13.** Ultrastructural morphology of glioblastoma stem-like cells (GSCs). Apoptotic GSCs with pyknotic nucleus (n), degenerated mitochondria (white arrowheads), and swollen endoplasmic reticulum (star). Scale bar: 1 µm (a). Necrotic GSCs. Scale bar: 2 µm (b). Nucleus (asterisks), degenerated mitochondria (black arrows), ruptured plasma membranes (white arrowheads), blebbing of apoptotic body (black arrowhead), intermediate junctions or desmosomes (black circles), and lipid droplets (black rectangle).

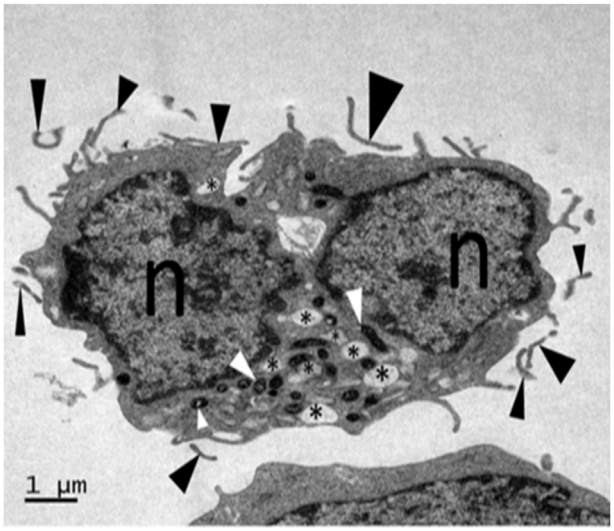


**Figure 14.** Two glioma stem-like cells (GSCs) with mitochondria-associated membranes after 3 d of nutrient starvation, possessing sporadic cytoplasm with degenerated mitochondria (white arrowheads). GSCs with nucleus (n) separated into two regions. Swollen endoplasmic reticulum (asterisks) can be seen. Microvilli (black arrowheads) are seen to be separated from GSCs.

possessed multiple MAMs. Furthermore, on day 3 of nutrient starvation, we observed close associations between two or three swollen, rugous ER profiles and damaged mitochondria (Figure 10). Additionally, GSCs possessed a "MAM network" involving 15 direct inter-organellar close associations between mitochondria linked to expanded ERs. GSCs, also displaying a "MAM network," were adjacent to nuclei and possessed swollen ER profiles and electron-dense vacuoles, damaged mitochondria, or mitophagy (Figures 11 and 12). Apoptotic gliosphere stem cells had pyknotic or necrotic nuclei, degenerated mitochondria, and swollen ER (Figure 13). On day 3 of nutrient starvation, we also observed two GSCs with MAM with sporadic cytoplasm containing degenerated mitochondria. Glioma stem cells of the nuclei were separated into two regions and contained swollen ER. Microvilli were distinct from GSCs (Figure 14).

### *3.4. Effects of nutrient starvation on cleaved caspase-3, phospho-beclin 1, LC 3B-I, and LC 3B-II expression*

Western blots revealed LC 3B I/II expression and beclin 1 phosphorylation (Figure 15). The latter appears to play a role in autophagy by regulating *UVRAG* (ultraviolent irradiation resistance-associated gene), which encodes a protein that forms a complex with VPS34 (vacuolar protein sorting 34), ATG 14 L, and LC 3B I/II in GSCs after starvation for 1, 3, 4, and 5 d. Western blots confirmed the mechanism of apoptosis as cleaved caspase-3 leading to apoptosome formation in C6 GSCs after days 1 and 3 of starvation treatment.

## 4. Discussion

This study successfully used the C6 gliosphere as an experimental model to represent GSCs. Nutrient starvation decreased proliferation by 60–81% in the surviving fraction of C6 GSCs, while increasing apoptosis by 99.9% and autophagy by 94.6%. Starved cells exhibited a higher proportion of early and late apoptotic cell death, as well as non-apoptotic cell death, compared with control GSCs. Similarly, previous research demonstrated that combining metformin and 9-cis retinoic acid decreased GSC proliferation rate and increased apoptosis by 86% in vitro [17]. Furthermore, metformin in combination with temozolomide induced 62.73% early and 61.73% late apoptosis in U87 GSCs [17, 18]. After 3 d of nutrient starvation, C6 GSCs exhibited shrinking, membrane blebs, cytoplasmic vacuolization, and pyknotic nuclei, all characteristic of early apoptosis. As indicators of late apoptosis, we observed apoptotic bodies and nuclear fragments in higher numbers. Currently, drug-induced apoptosis may occur via glutamine starvation reducing GSC proliferation (glutamate pathway) [19], or the mitochondria pathway [20, 21].

We speculate that nutrient starvation first induced functional changes in mitochondria that eventually triggered apoptosis and autophagy in GSCs. Normally, GSCs have fewer mitochondria and ER in cytoplasm than non-GSCs [22]. When gliospheres lack glucose, glutamine, and calcium, the reverse occurs, suggesting that starvation stresses the cells and increases free radicals. Cell stress opens more channels (MAMs) between mitochondria and ER [23]. Gaps between MAMs cause protein breakdown through autophagy or mitophagy to eliminate deteriorated cells. Nutrient starvation increases beclin 1 phosphorylation and LC3 I/II expression through autophagic phagosomes in the mitochondria and ER. Western blots detected both apoptosis and autophagy markers in C6 GSCs after nutrient starvation. Beclin-1 phosphorylation may be an autophagy marker because of its role in autophagosome maturation by regulating the UVRAG-VPS34 complex that contains ATG 14 and LC 3B I/II in gliosphere stem cells. We were also able to demonstrate that the mechanism of apoptosis involves cleaved caspase-3 generating the apoptosome in C6 GSCs. Specifically, nutrient starvation promotes the movement of Bax or Fas-L to the membrane, triggering the release of cytochrome c from the mitochondria. This step, in turn, activates caspase-3, leading to apoptosis.

Nutrient starvation decreases intracellular ATP/AMP ratio, thereby activating AMPK to suppress the mammalian target of rapamycin complex (mTOR) pathway and induce growth arrest, apoptosis, and autophagy [15]. Some studies reported that nutrient starvation decreases proliferation, blocks G0/G1 cell cycle progression, and induces cell death in GSCs through AMPK-dependent inhibition of FOXO3 and AKT [16]. In contrast, AMPK is active in gliomas and the autophagic effects of starvation on GSCs are AMPK-independent, involving the upregulation of LC3, binding of phospho-beclin 1 to ATG14L and hVPS34, and fusion of lysosomes to form autophagosomes [16, 24]. Using CD 133-positive glioma cells can help reduce apoptosis and stop autophagy after nutrient deprivation [25]. The more complex proliferation and

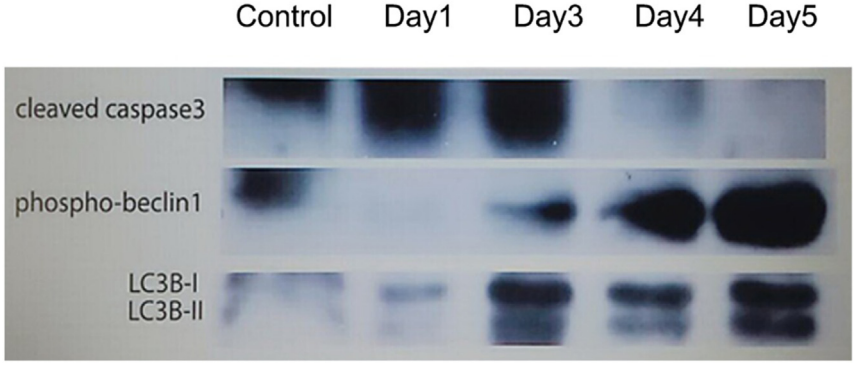


**Figure 15.** Representative Western blot detecting cleaved caspase-3 (apoptosis marker) and phospho-beclin 1, LC 3B-I, LC 3B-II (autophagy markers) in C6 glioma stem-like cells (GSCs) after nutrient starvation for 1, 3, 4, and 5 d. Beclin-1 phosphorylation may play a role in autophagy by regulating *UVRAG* (ultraviolent irradiation resistance-associated gene), which encodes a protein that forms a complex with VPS34 (vacuolar protein sorting 34), ATG 14 L, LC 3B I/II in GSCs after starvation for 1, 3, 4, and 5 d. Western blots confirmed the mechanism of apoptosis as caspase-3 cleavage leading to apoptosome formation in C6 GSCs after day 1 and 3 of starvation treatment.

differentiation of GSCs (into neurons, astrocytes, and oligodendrocytes) are unlike CD 133-positive glioma cells. The lack of glucose, glutamine, and calcium inhibited GSCs from generating glycolytic products to fuel other biosynthetic pathways, such as the pentose phosphate pathway [26] and lipid or amino acid biosynthesis. This process suppresses glutathione synthesis directly, while indirect suppression also occurs through an increase in cysteine, which causes mitochondrial dysfunction and cellular damage [27, 28].

Both the glutamate pathway and the mitochondria pathway induces apoptosis and autophagy. Normally, undifferentiated GSCs have fewer MAMs than differentiated GSCs. Nutrient starvation appears to further increase MAMs in GSCs, while also generating abnormal mitochondria and swollen ER. Accumulation of MAMs, swollen ERs, and abnormal mitochondria could lead to the formation of "disrupting invadopodia,'' which could then stimulate a proportion of GSCs to become non-GSCs that lack a nucleus [29]. Formation of disrupting invadopodia could form the basis of a novel noninvasive cancer treatment that induces ER stress to trigger cancer cell apoptosis and autophagy.

Our findings are in line with many previous reports indicating that nutrient starvation affects metabolic reactions in mitochondria of cancer cells. This study provides further evidence that nutrient starvation affects GSCs [17, 18, 19, 24] as rapidly as within 72 h. The data have implications for cancer therapy and could potentially be applied in clinical trials. Future studies could examine the effects of nutrient starvation on other molecular mechanisms in GSCs, such as Notch, Hedgehog, and Wnt/β-catenin pathways. Additionally, research on nutrient starvation can expand to include other methods for inducing the condition, including combining metformin and 9-cis retinoic acid, or metabolic reprogramming [17, 30].

## 5. Conclusions

This study subjected GSCs nutrient starvation, then detected apoptosis and autophagy markers using western blots. By day 5, nutrient starvation decreased proliferation by about 81.5% and induced almost 100% cell death through apoptosis and autophagy. However, even on day 1, we observed autophagy (99.7%) and apoptosis (35.1%) of GSCs. After 3 days, autophagy percentage remained the same while apoptosis rose to 96.1%. Thus, gliospheres were reduced by about 81.5% on day 5. We demonstrated that nutrient starvation increased both early and late apoptosis in C6 GSCs. Moreover, our morphological analyses revealed that mechanisms of autophagy and apoptosis involve damaged mitochondria and expanded ER contact sites (MAM) in the cytoplasm (disrupting invadopodia). The process of disrupting invadopodia could form the basis of novel anti-cancer therapy that focuses on metabolic changes. In conclusion, our results provide novel insight into the role of nutrient starvation on inducing apoptosis and autophagy in GSCs.

## Declarations

### *Author contribution statement*

Wanna Sa-nongdej, Sukumal Chongthammakun: Performed the experiments; Analyzed and interpreted the data; Contributed reagents, materials, analysis tools or data; Wrote the paper.

Chanchai Songthaveesin: Conceived and designed the experiments; Performed the experiments; Analyzed and interpreted the data; Contributed reagents, materials, analysis tools or data; Wrote the paper.

### *Funding statement*

This work was supported by Faculty of Science, and Ramathibodi School of Nursing, Faculty of Medicine Ramathibodi Hospital, Mahidol University.

### *Data availability statement*

Data will be made available on request.

### *Declaration of interests statement*

The authors declare no conflict of interest.

### *Additional information*

No additional information is available for this paper.

## References

[1] P.D. Robles, K.M. Fiest, A.D. Frolkis, T. Pringsheim, C. Atta, C.S. Germaine-Smith, L. Day, D. Lam, N. Jette, The worldwide incidence and prevalence of primary brain tumors: a systematic review and meta-analysis, Neuro Oncol. 17 (2015) 776–783.
[2] J. Miska, M.S. Lesniak, Neural stem cell carriers for the treatment of glioblastoma multiforme, EBioMedicine 2 (2015) 2774–2775.
[3] M. Jackson, F. Hassiotou, A. Nowak, Glioblastoma stem-like cells: at the root of tumor recurrence and a therapeutic target, Carcinogenesis 36 (2015) 177–185.
[4] B. Auffinger, D. Spencer, P. Pytel, A.U. Ahmed, M.S. Lesniak, The role of glioma stem cells in chemotherapy resistance and glioblastoma multiforme recurrence, Expert Rev. Neurother. 15 (2015) 741–752.
[5] I. Chiodi, G. Picco, C. Martino, C. Mondello, Cellular response to glutamine and/or glucose deprivation in vitro transformed human fibroblasts, Oncol. 41 (2019) 3555–3564.
[6] O. Warburg, On the origin of cancer cells, Science 123 (1956) 309–314.
[7] K.E. Jung, K.O. Ran, H.S. Won, P.S. Hye, K. Hyungge, Glioma stem cells and their non-stem differentiated glioma cells exhibit differences in mitochondrial structure and function, Oncol. Rep. 39 (2017) 411–416.
[8] I.S. Mathiasen, I.N. Sergeev, L. Bastholm, F. Elling, A.W. Norman, M. Jäättelä, Calcium and calpain as key mediators of apoptosis-like death induced by vitamin D compounds in breast cancer cells, J. Biol. Chem. 277 (2002) 30738–30745.
[9] I.N. Sergeev, Calcium as a mediator of 1,25-dihydroxyvitamin D3-induced apoptosis, J. Steroid Biochem. Mol. Biol. 89–90 (2004) 419–425.
[10] A.L. Edinger, C.B. Thompson, Death by design: apoptosis, necrosis and autophagy, Curr. Opin. Cell Biol. 16 (2004) 663–669.
[11] I. Ghobrial, T.E. Witzig, A.A. Adjei, Targeting apoptosis pathways in cancer therapy, CA Cancer, J. Clin. 55 (2005) 178–194.
[12] M.O. Hengartner, The biochemistry of apoptosis, Nature 407 (2000) 770–776.
[13] I. Herr, K.M. Debatin, Cellular stress response and apoptosis in cancer therapy, Blood 98 (2001) 2603–2614.
[14] S.W. Lowe, A.W. Lin, Apoptosis in cancer, Carcinogenesis 21 (2000) 485–495.
[15] S. Alers, A.S. Löffler, S. Wesselborg, B. Stork, Role of AMPK-mTOR-Ulk1/2 in the regulation of autophagy: cross talk, shortcuts, and feedbacks, Mol. Cell Biol. 32 (2012) 2–11.
[16] M. Chiao, W. Cheng, Y. Yang, C. Shen, J. Ko, Suberoylanilide hydroxamic acid (SAHA) causes tumor growth slowdown and triggers autophagy in glioblastoma stem cells, Autophagy 9 (2013) 1509–1526.
[17] C. Songthaveesin, W. Sa-nongdej, T. Limboonreung, S. Chongthammakun, Combination of metformin and 9-cis retinoic acid increases apoptosis in C6 glioma stem-like cells, Heliyon 4 (5) (2018), e00638.
[18] Z. Yu, G. Zhao, P. Li, Y. Li, G. Zhou, Y. Chen, G. Xie, Temozolomide in combination with metformin act synergistically to inhibit proliferation and expansion of glioma stem-like cells, Oncol. Lett. 11 (2016) 2792–2800.
[19] T. Saverio, O. Anaïs, A. Shafiq, F. Fred, K. Olivier, Z. Liang, M. Hrvoje, S.P. Øystein, W. Adam, W. Allon, L. Susan L, H. Andreas K, B. Susan C, R. Eytan, M.S. Harald, J.M. Lund, C. Anthony J, B. Rolf, N. Simone P, G. Eyal, Glutamine synthetase activity fuels nucleotide biosynthesis and supports growth of glutamine-restricted glioblastoma, Nat. Cell Biol. 17 (2015) 1556–1592.
[20] P. Wilhelm, T. Craig B, Nutrient acquisition strategies of mammalian cells, Nature 546 (2017) 234–242.
[21] S. Fulda, K.-M. Debatin, Extrinsic versus intrinsic apoptosis pathways in anticancer chemotherapy, Oncogene 25 (2006) 4798–4811.
[22] G. Arismendi-Morillo, A. Castellano-Ramírez, T.N. Seyfried, Ultrastructural characterization of the mitochondria-associated membranes abnormalities in human astrocytomas: functional and therapeutics implications, Ultrastruct. Pathol. 41 (2017) 234–244.
[23] M. Hamasaki, N. Furuta, A. Matsuda, A. Nezu, A. Yamamoto, N. Fujita, H. Oomori, T. Noda, T. Haraguchi, Y. Hiraoka, A. Amano, T. Yoshimori, Autophagosomes form at ER-mitochondria contact sites, Nature 495 (2013) 389–393.
[24] L. Shang, S. Chen, F. Du, S. Li, L. Zhao, X. Wang, Nutrient starvation elicits an acute autophagic response mediated by Ulk1 dephosphorylation and its subsequent dissociation from AMPK, Proc. Natl. Acad. Sci. U.S.A. 108 (2011) 4788–4793.
[25] S. Haojie, Z. Mingzhi, C. Kai, L. Peng, H. Shou, L. Ruizhi, S. Ming, Z. Wotan, L. Jinen, G. Jinhai, L. Yihan, Z. Xiaoyan, H. Qihua, S. Li, Resistance of glioma cells to nutrient-deprived microenvironment can be enhanced by CD 133-mediated autophagy, Oncotarget 7 (2016) 76238–76249.
[26] T. Mayumi, N. Osamu, T. Seiji, O. Mitsuyo, Y. Toshifumi, I. Takatsugu, S. Eiji, O. Nobuyuki, Y. Takehiro, Y. Hiroshi, S. Makoto, S. Hideyuki, Modulation of

glucose metabolism by CD44 contributes to antioxidant status and drug resistance in cancer cells, Cancer, Res. 72 (2012) 1438–1448.
[27] I. Chiodi, G. Picco, C. Martino, C. Mondello, Cellular response to glutamine and/or glucose deprivation in in vitro transformed human fibroblasts, Oncol. Rep. 41 (2019) 3555–3564.
[28] J.S. Carew, P. Huang, Mitochondrial defects in cancer, Mol. Canc. 1 (2002) 1–12.
[29] G. Arismendi-Morillo, N.T. Hoa, L. Ge, M.R. Jadus, Mitochondrial network in glioma's invadopodia displays an activated state both in situ and in vitro: potential functional implications, Ultrastruct. Pathol. 36 (2012) 409–414.
[30] W. Patrick, T. Craig, Metabolic reprogramming: a cancer hallmark even warburg did not anticipate, Canc. Cell 21 (2012) 297–308.